Particle Accelerators, 1988, Vol. 23, pp. 227–237
Reprints available directly from the publisher
Photocopying permitted by license only

Printed in the United States of America

COMPUTER SIMULATION OF PHASE MOTION IN THE CW RACETRACK MICROTRON

V. K. GRISHIN, B. S. ISHKANOV, M. A. SOTNIKOV, and V. I. SHVEDUNOV

Institute of Nuclear Physics, Moscow State University, 119899 Moscow, USSR

(Received September 9, 1986; in final form June 8, 1987)

An approach to phase-motion analysis in the racetrack microtron (RTM) is proposed. The approach is based on the notion of an asymptotically synchronous particle. The RTM separatrix is studied as a function of injection energy, fringing field of the bending magnets, and distance between magnets. The acceptance values for injected energies of 5, 7, and 9 MeV are $\sim 6.2/\pi$ MeV · deg, $\sim 8.8/\pi$ MeV · deg, and $\sim 9.5/\pi$ MeV · deg, respectively. (The parameters of the RTM designed at the Institute of Nuclear Physics, Moscow State University, were used in the calculations.) The preferred initial conditions providing the beam with a given monochromaticity at the RTM output are suggested. Calculations show that, in order to obtain a 10^{-4} monochromaticity of the final beam, the longitudinal emittance should be ~ 5 keV · deg, i.e., 0.2% of the acceptance, and the ellipse formed by the RTM injection system should have the corresponding axis inclination in phase space.

Different factors affecting the RTM beam monochromaticity, such as transverse particle motion, radial and time dependence of the accelerating field, inhomogeneity, and instability of the bending magnet field, are estimated. It is shown that the nonlinear distortions of the beam phase shape for $\Delta B/B = \pm 10^{-3}$ lead to more stringent requirements for the longitudinal emittance.

1. INTRODUCTION

CW racetrack microtron (RTM) is being designed and manufactured at the Institute of Nuclear Physics, Moscow State University.[1] A schematic drawing of the accelerator is shown in Fig. 1, and the main parameters of the accelerator are listed in Table I.

The CW RTM with a maximum final energy between 100 and 200 MeV[2–6] differs in some respects from the more fully studied pulsed RTM.[7–11] (For a complete survey of different RTM projects see Ref. 12.) The principal differences are accounted for by the low intensity of the linac accelerating field (1–1.5 MeV/m), which necessitates, first, a large separation between the bending magnets and, second, the 5–15 MeV injection system.

The high average beam current of the CW RTM requires that the particle losses in the acceleration process be minimized. This minimization is accomplished by properly matching the injected beam emittance and the RTM acceptance. When an output beam with an energy spread of $\pm 10^{-4}$ is needed, the requirements for matching the injected-beam parameters to the RTM separatrix are even more stringent. At present these problems are given little attention in the literature.

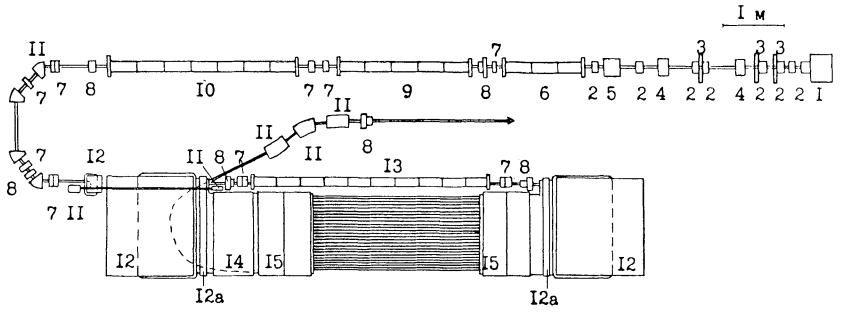

FIGURE 1 The CW racetrack microtron under construction at the Institute of Nuclear Physics, Moscow State University; 1—electron gun; 2—magnetic lens; 3—collimator; 4—rf deflection cavity; 5—bunching resonator; 6—graded β section; 7—quadrupole singlets and doublets; 8—rf beam monitor; 9,10—linacs with $\beta = 1$; 11—sector bending magnet; 12—180° bending magnets; 12a—opposite poles; 13—main linac with $\beta = 1$; 14—ejection chamber; 15—vertical and horizontal steerers.

In most cases (see, for example, Refs. 2 and 13), phase motion is analyzed using equations of phase and energy oscillations with respect to the phase and energy of a hypothetical particle with velocity equal to that of light. In this paper a different approach, based on the notion of an asymptotically synchronous particle, is suggested. This approach simplifies the choice of initial conditions in order to obtain a beam with preset output properties.[14]

TABLE I

Parameters of the Racetrack Microtron at the Institute of Nuclear Physics, Moscow State University

Injection energy, E_{inj} (MeV)	7
Final energy, E_{output} (MeV)	118
Energy gain, ΔE (MeV)	4.43
Number of orbits, N	25
Operating frequency, f (MHz)	2450
Synchronous phase, ψ_s (deg)	106
Incremental number of wavelengths per orbit, ν	1
Magnetic field value, B_0 (T)	0.76
Diameter of last orbit, d_{25} (cm)	105
Average beam current, I (μA)	100
Energy spread, $\Delta E/E$	10^{-3}–10^{-4}
Transverse emittance of the output beam, ε_T(π mm-mrad)	0.05
Accelerating structure length, L(m)	4.16
Effective shunt impedance, R_e (MΩ/m)	75
Total rf power including the injection system, P (kW)	175

2. EQUATIONS OF PHASE MOTION IN THE RACETRACK MICROTRON

The behavior of the phase and energy of particles during acceleration in a RTM with a standing-wave linear accelerator obeys the equations

$$\psi(n) = \psi(n-1) + \frac{2\pi}{\lambda}\left[\sum_{m=1}^{M}\int_{-\lambda/4}^{\lambda/4}\frac{dz}{\beta_{n-1}^{m}(z)} + \frac{\mathscr{L}(n-1)-L}{\beta_{n-1}}\right], \tag{1a}$$

$$E(n) = E(n-1) + e\sum_{m=1}^{M}\int_{-\lambda/4}^{\lambda/4}\mathscr{E}_m(z)\cos\left[\frac{2\pi}{\lambda}\int_{-\lambda/4}^{\lambda/4}\frac{dZ'}{\beta_{n-1}^{m}(z')} + \psi(n-1)\right]dZ. \tag{1b}$$

Here $\psi(n)$ and $E(n)$ are, respectively, the particle phase with respect to the rf field phase and the particle output energy at the start of the nth orbit, where $n = 1, 2, \ldots, N$, and N is the total number of orbits. The first expression in brackets accounts for the phase slip in the linac and the second expression in brackets [Eq. (1a)] accounts for the phase slip, in the bending magnets, the drift space, and the fringing fields of the magnets, L is the linac length containing M cells ($L = M\lambda/2$), λ is the rf-field wavelength in free space, $\mathscr{L}(n)$ is the total orbit length, and $\beta_n^m(z)$, β_n is the relative electron velocity. The second term in the right-hand side of Eq. (1b) accounts for the energy gain per turn. $\mathscr{E}_m(z)$ is the electric-field amplitude on the mth cell axis, and $\psi(0)$ and $E(0)$ correspond to the phase and energy of an injected particle, respectively. With the chosen phase reference point, the maximum energy gain of an ultrarelativistic electron is obtained for $\psi(n) = \pi/2$.

The orbit length of a particle moving parallel to the linac axis can be represented as

$$\mathscr{L}(n) = 2S + 2\pi R(n) + \Delta S_M(n), \tag{2}$$

where S is the distance between the edges of ideal bending magnets (magnets without fringing field), $R(n)$ is the turn radius of a particle in the magnet, and $\Delta S_M(n)$ is the difference in the orbit length between the real and ideal magnets.

In the ultrarelativistic limit ($\beta_n = 1$), one can introduce the notion of a synchronous particle with the condition of resonance motion:

$$2S + 2\pi R(n) + \Delta S_M = \lambda[\mu + \nu(n-1], \tag{3}$$

where $\Delta S_M = \lim_{\beta_n \to 1} \Delta S_M(n)$, and ν is the incremental number of wavelengths per turn. In this limit the relation of the synchronous energy gain ΔE_s and the magnetic-field induction B_0 in the bending magnets is

$$B_0 = \frac{2\pi\,\Delta E_s}{\lambda \nu c e}, \tag{4}$$

where, for zero beam current,

$$\Delta E_s = \sqrt{PR_e L}\cos(\psi_s - \pi/2), \tag{5}$$

where ψ_s is the synchronous phase, P is the dissipated power in the linac, and R_e is the effective shunt impedance.

In this approximation Eqs. (1a) and (1b) lead to the equations of phase oscillations of a classical microtron (CM) whose basic properties are well known.[15–17] The validity of the approximation $\beta_n = 1$ is determined mainly by the relation of particle velocity and the distance between magnets. That is, the phase shift of a particle in the drift space $\Delta\varphi_D$ must be much less than the width of the CM phase-stable region, specifically for ψ_s at the center of linear stability band

$$\Delta\varphi_D(n) = \frac{2S(1-\beta_n)}{\beta_n} \cdot \frac{360^\circ}{\lambda} \lesssim 1^\circ. \tag{6}$$

For the CW RTM at 100–200 MeV, Eq. (6) starts to be fulfilled at 40–50 MeV; i.e., the results of the phase-motion analysis for the CM are acceptable for most orbits. However, in the first few orbits the phase shift is tens of degrees, the ultrarelativistic approximation is inapplicable, and synchronous particles, in the strict sense, are nonexistent.

Let an asymptotically synchronous particle in the RTM be a particle whose phase behavior satisfies the condition

$$\lim_{\beta_n \to 1} \psi_s(n) = \psi_s. \tag{7}$$

The properties of equations of the CM phase oscillations and the Liouville theorem suggest the existence of the single trajectory on the phase plane with the initial point ψ_s (0), E_s (0) satisfying Eq. (7). To search for the phase path of the synchronous particle ψ_s (n), E_s (n), $n = 0, \ldots, N$, the following procedure is suggested:

1. The parameters ΔE_s, B_0, ψ_s, and ν are chosen in the ultrarelativistic limit. The maximum width of the phase-stable region with the inclusion of nonlinear resonance[12,17,18] is provided by the following values; $\nu = 1$, $\psi_s \simeq 106^\circ$. The terms ΔE_s and B_0 are determined by Eqs. (5) and (4), respectively.

2. The free parameter that enables one to match the $E_s(0)$ value of the synchronous-phase path and the injected-beam energy is the separation between magnets S. The functional connection of $E_s(0)$ and S is given by Eq. (7) and Eqs. (1a) and (1b). The search for the phase path satisfying Eq. (7) at a sufficiently large yet finite number of orbits, N, can be reduced to the search for the minimum value of $\delta\psi_N = \bar{\psi}(N) - \psi_s$, depending on the values of $\psi(0)$ and S for a given $E_s(0)$, by means of a numerical solution of Eqs. (1a) and (1b). The bar above $\psi(N)$ means that $\psi(N)$ is averaged over the period of phase oscillations.

This procedure can also be used when tuning the real accelerator with the signal of the rf phase monitor located on the linac axis (Fig. 1). In certain cases it is desirable to vary the energy of an injected beam rather than the distance between magnets.

3. CALCULATIONS OF THE RTM SEPARATRIX

The bunches of particles injected into the RTM occupy the non-vanishing area on the phase plane (they have a nonzero longitudinal emittance ε_L). In this connection the analysis of phase motion in the RTM has the following three goals: (1) calculating the separatrix and optimizing the longitudinal acceptance; (2) matching the center of the beam phase-space distribution to the phase-plane point $E_s(0)$, $\psi_s(0)$; (3) matching the axial inclination of the beam phase-space distribution with the RTM separatrix.

After solving these problems, we formulate the requirements for the injected beam in order to minimize losses in the acceleration process at large ε_L, minimize the nonlinear distortions and attain high monochromaticity at small ε_L, and obtain tolerances on different RTM parameters.

We have developed a numerical-analysis program of RTM phase motion that enables one to obtain the phase path of a synchronous particle for a given injection energy, to determine the form and location of the separatrix, to obtain the longitudinal acceptance, and to calculate the injected-beam parameters needed to obtain a preset monochromaticity at the RTM output. The beam phase-space distribution given below was obtained as a result of the analysis of phase trajectories of a large ensemble of particles (about 10^4). To speed up the calculation, the preliminary integration of phase-motion equations in the linac and in the fringing fields of the bending magnets has been carried out on the detailed mesh with variable step in energy-phase plane. The particle energy and phase values at the outlet of the elements were determined with the help of second-order interpolation of the entrance values.

Calculations were carried out on a 32-bit computer with double precision. According to our estimates, the relative accuracy of energy and phase determination at the end of the 25th orbit is 10^{-5}–10^{-6} and 0.1°–0.01°, respectively. The calculation results presented below are obtained from the CW RTM at the Institute of Nuclear Physics, Moscow State University; the parameters of this RTM are listed in Table I. At the same time these results are general in nature and can be used to evaluate other projects.

In Fig. 2 the separatrix computations for the RTM with 25 orbits are illustrated. The simulation conditions and the acceptance values are listed in Table II. Figures 2A through 2C plots the separatrix versus injected energy. The fringing field of the bending magnets was compensated for by the reversed field in order to obtain an infinite-edge focal length in the vertical plane.[19] The reversed-field maximum was ~7 cm from the physical edge of the magnet, its value being 30% of the main field. The magnet-gap width was 6 cm. The acceptances (ξ) for injected energies of 5, 7, and 9 MeV are $\xi \simeq 6.2/\pi$ MeV · deg, $\xi \simeq 8.8/\pi$ MeV · deg, and $\xi \simeq 9.5/\pi$ MeV · deg, respectively. Figure 2D presents the CM separatrix $\xi \simeq 10.7/\pi$ MeV · deg. As can be seen, the RTM acceptance is quite large. As the injected energy decreases, the acceptance gets smaller, and the RTM separatrix departs from the CM separatrix. At a certain injected energy (in this case $E(0) \simeq 3.5$ MeV), the acceptance goes to zero. Motion without phase correction becomes impossible.

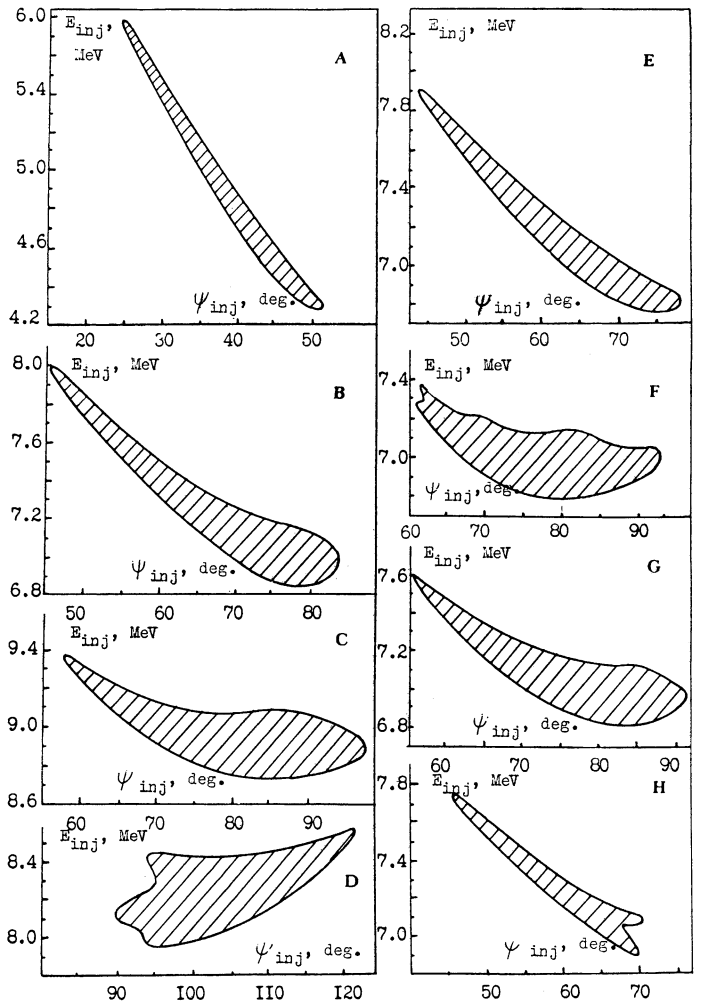

FIGURE 2 Form and value of the acceptance of the 25-orbit RTM plotted versus different parameters from Table II.

The role of the fringing fields of the bending magnets is demonstrated in Figs. 2E and 2F, where the RTM separatrix at an injected energy of 7 MeV is given for the bending magnet without compensation of the fringing field ($\xi \simeq 6.4\pi$ MeV · deg) and for the ideal magnet $\xi \simeq 9.3/\pi$ MeV · deg). Figure 2G shows the RTM separatrix with a 4.4-m distance between the magnets. In this case $\xi \simeq 9/\pi$ MeV · deg.

The particles falling inside the limits of the separatrix domain must travel through all N orbits to have the RTM final-energy spread obtainable in a first approximation by the formula

$$\Delta E/E \simeq \pm \mathrm{tg}\,(\psi_s - \pi/2)\,\Delta\psi/N, \tag{8}$$

TABLE II

The Separatrix Area as a Function of Different Parameters of the RTM after 25 Orbits

Fig. 2 reference	Injection energy (MeV)	Distance between magnets (m)	Character of the drop of the fringing field of the bending magnets	Path-length difference in magnet from the ideal (ΔS_M, mm)	Separatrix area (MeV · deg)
A	5	6	Compensation of	-10.5×2	6.2
B	7	6	fringing field	-10.5×2	8.8
C	9	6	by opposite pole	-10.5×2	9.5
D	8.2	0	CM	0	10.7
E	7	6	Without compensat.	39.9×2	6.4
F	7	6	Ideal magnet	0	9.3
G	7	4.4	With compensation	-10.5×2	9.0
H	7	6	With compensation $\Delta B/B = 10^{-3}$	-10.5×2	4.4

where $\Delta\psi$ is the half width of phase-stable region. For $\psi_s = 106°$, $N = 25$, $\Delta E/E \simeq \pm 3\ 10^{-3}$, to attain $\Delta E/E \simeq \pm 10^{-4}$, the particles should be within $\Delta\psi \leq \pm 0.5°$, provided that the center of the beam phase-space distribution coincides with the coordinates of a synchronous trajectory.

To properly choose the initial conditions to obtain a specified value of $\Delta E/E$ at the RTM output, we have simulated the separatrix and determined the average deviation of phases and energies over all orbits from the synchronous values

$$\delta\psi = \frac{1}{N}\sum_{n=1}^{N}[\psi(n) - \psi_s(n)],$$
$$\delta E = \frac{1}{N}\sum_{n=1}^{N}[E(n) - E_s(n)]. \tag{9}$$

Figure 3A presents the levels of equal δE in the coordinate axes $\psi(0)$, $E(0)$ for an injection energy of 7 MeV. As can be seen, to obtain high monochromaticity the beam phase-space distribution should be nearly elliptical.

Representing the equation of the envelope of beam phase-space distributions as

$$\gamma\,\Delta\psi^2 + 2\alpha\,\Delta E\,\Delta\psi + \beta\,\Delta E^2 = \varepsilon, \tag{10}$$

where ε is the beam emittance, and working from Fig. 3A, we have determined the parameters of an ellipse needed to obtain a given δE value. These parameters are listed in Table III.

The maximum deviation of particle energy from the synchronous value on any orbit will not be greater than $\pi/2 \cdot \delta E$, because the oscillation amplitude does not vary. Thus, in order to obtain the $\pm 10^{-4}$ monochromaticity of the final beam, the longitudinal emittance should be $\varepsilon \approx 5$ keV · deg, i.e., 0.2% of the acceptance, and the parameters of the ellipse formed by the RTM injection system should correspond to the parameters listed in Table III. For comparison, Fig. 3B gives the analogous results for the classical microtron.

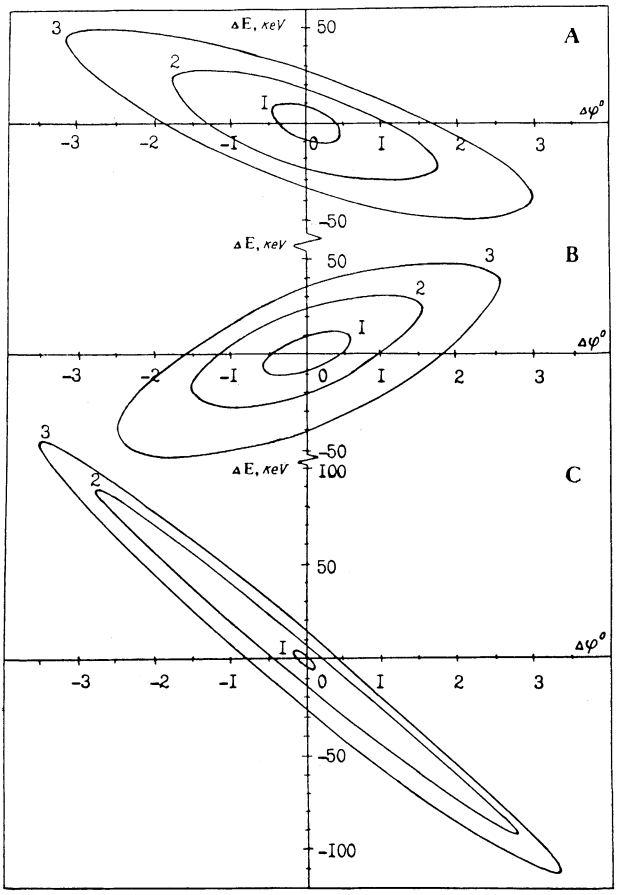

FIGURE 3 Levels of equal deviations of energy δE from the synchronous values for the computation conditions listed in Table III.

4. THE PERTURBING FACTORS

In this section we consider some factors affecting the phase motion in the RTM. One of the essential factors is the transverse motion of particles in the RTM. The orbit length of a particle moving at an angle $\theta(n)$ to the linac axis differs from that of a particle with $\theta(n) = 0$ by

$$\Delta\mathscr{L}(n) = 2R(n) \cdot \theta(n) + S \cdot \theta^2(n). \tag{11}$$

The total phase shift of this particle after N orbits depends on the transverse emittance of a beam and the focusing scheme. With the focusing elements on the RTM common axis and the transverse emittance $\simeq 0.5$ mm mrad at 7 MeV, the phase shift after 25 orbits is of the order of 1°, which corresponds to $\Delta E/E \simeq \pm 2 \cdot 10^{-4}$. With the focusing elements on the return orbits, the phase shift is 10°; besides, resonance phenomena are possible here when the phase-

TABLE III

Parameters of Ellipses Needed to Obtain a Given Average-Energy-Deviation Value from Synchronous Values

Fig. 3 reference	Computation parameters	No. of ellipse	$\delta(E)$, (keV)	emittance, ε (keV · deg)	Parameters of ellipses α	β	γ
A	Racetrack microtron with 25 orbits, $S = 6$ m	1	10	6.18	0.403	0.057	20.40
		2	20	38.8	0.845	0.071	24.03
		3	30	87.7	0.890	0.079	22.80
B	Classical microtron with 25 orbits	1	10	4.59	−0.60	0.055	24.91
		2	20	37.0	−1.38	0.093	31.10
		3	30	110.8	−1.47	0.088	35.80
C	Racetrack microtron with 25 orbits, $\Delta B/B = 10^{-3}$	1	10	0.30	1.477	0.052	61.2
		2	20	27.75	9.204	0.278	308.3
		3	30	72.45	5.658	0.164	201.3

oscillation period is close to that of betatron oscillations. The resonance phenomena lead to an unlimited growth of betatron and phase-oscillation amplitudes.[20,21]

Thus, the results of the phase-motion analysis for particles on the central trajectory hold true for weak focusing. When the quadrupole lenses are on the return orbits, the longitudinal and transverse motions must be analyzed jointly.

One more factor contributing to the connection of longitudinal and transverse motion is the radial dependence of the accelerating field. For an accelerating structure with a 10-mm beam aperture, the difference in the effective shunt impedance, which determines the energy gain of a particle in the central trajectory and a particle shifted by 3 mm with respect to the axis, is $\Delta R_e/R_e \simeq 10^{-2}$.[14] If the off-axis shift is retained in the acceleration process, the difference in R_e at a given magnetic field is equivalent to the change in the synchronous phase. This results in phase oscillations of the particles with $E(0) = E_s(0)$, $\psi(0) = \psi_s(0)$ at the instant of injection, which leads to spectrum broadening at the RTM output:

$$\Delta E/E = \pm \frac{\operatorname{tg}(\psi_s - \pi/2)}{N} \cdot \frac{\Delta R_e}{2R_e} \simeq \pm 6 \times 10^{-5}. \tag{12}$$

The accelerating-field instability in the linac can also be characterized by the equivalent change of the synchronous phase but only if the transient time substantially exceeds the time of particle motion through all orbits (for $N = 25$, $t \cong 1$ nsec). In this case the instability should be less than $\pm 1\%$ in order that $\Delta E/E \leqslant \pm 10^{-4}$ at $N = 25$. The phase shift of a particle per turn due to

inhomogeneity of the field of the bending magnets is[2]

$$\Delta\psi_n \simeq \frac{\Delta B}{B} \cdot \frac{2\pi l_n}{\lambda}, \tag{13}$$

where l_n is the orbit length in the magnetic field.

We have calculated the separatrix when the phase shifts due to field inhomogeneity are the same for all particles within one bunch and are summed randomly over orbits. The results for $\Delta B/B = \pm 10^{-3}$ are shown in Fig. 2H ($\xi \simeq 4.4/\pi$ MeV · deg). It should be emphasized that the magnetic-field inhomogeneity excludes the fulfilment of Eq. (7): the synchronous particle oscillates with a large amplitude and, thus, leaves the modified-separatrix domain. Figure 3C illustrates the separatrix simulation and shows the levels of equal deviation in energy δE with respect to the particle that was at the center of the modified separatrix on the last orbit. The resulting phase-space distribution brings about more stringent requirements to the longitudinal emittance for $\Delta E/E = \pm 10^{-4}$. The choice of initial conditions becomes more complicated.

The large oscillation amplitude of the center of the beam phase space leads to the irregularity of the RTM orbital spacing,[10] which makes it difficult to place quadrupoles on the return orbits.

As for the time behavior of the magnetic field, the requirement that the magnetic field be stable is directly connected with the requirement that the beam be monochromatic to obtain $\Delta E/E = \pm 10^{-4}$, $\Delta B/B = \pm 10^{-4}$.

5. CONCLUSIONS

The main results of the present work are:

1. An approach to RTM phase-motion analysis is proposed. The approach is based on the notion of an asymptotically synchronous particle.
2. The RTM separatrix is studied as a function of injection energy and fringing field of the bending magnets.
3. The preferred initial conditions for providing the beam with a given monochromaticity at the RTM output are suggested.
4. Different factors affecting the RTM beam monochromaticity are estimated.

REFERENCES

1. Yu. I. Gorbatov, V. K. Grishin, B. S. Ishkhanov, M. Yu. Nikolskii, I. M. Piskarov, V. M. Sorvin, M. A. Sotnikov, V. I. Shvedunov, A. N. Sandalov, A. V. Shumakov, and A. A. Kolomenskii, *The CW Racetrack Microtron of the Institute of Nuclear Physics, Moscow State University* (*Physical Substantiation*) (M. Izd. MGU, (1984), p. 84; *Proc. IX All Union Meeting on Charged Particle Accelerators, VII,* (Dubna, 1985), 129.
2. B. H. Wiik and P. B. Wilson, *Nucl. Instrum. Methods* **56,** 197 (1967).
3. P. Axel, A. O. Hanson, J. R. Harlan, R. A. Hoffswell, D. Jamnik, D. C. Sutton and L. M. Yonng, *IEEE Trans. Nucl. Sci.* **NS-22,** 1178 (1975).

4. H. Herminghaus, A. Feder, K. H. Kaiser, W. Manz, and H. v. d. Schmitt, *Nucl. Instrum Methods* **138,** 1 (1976).
5. S. Penner, R. I. Cutler, P. H. Debenham, E. R. Lindstrom, D. L. Mohr, M. A. D. Wilson, N. R. Yoder, L. M. Yonng, I. J. Boyd, E. A. Knapp, R. E. Martin, J. M. Potter, C. M. Schneider, D. A. Swenson, and P. J. Tallerico, *IEEE Trans. Nucl. Sci.* **NS-28,** 1526 (1981).
6. L. Cardman, *IEEE Trans. Nucl. Sci.* **NS-30,** 3267 (1983).
7. H. R. Froelch, A. S. Thompson, D. S. Edmonds, and J. J. Manca, *IEEE Trans. Nucl. Sci.* **NS-20**, 260 (1973).
8. V. I. Alexeev, K. A. Belovintsev, V. A. Boiko, R. M. Voronkov, A. I. Karev, and V. V. Kurakin, *Sov. J. Theor. Phys.* **46,** 2558 (1976).
9. M. A. Green, E. M. Rowe, W. S. Trzeciak, and W. R. Winter, *IEEE Trans. Nucl. Sci.* **NS-28**, 2074 (1981).
10. S. Rosander, M. Sedlacek, O. Wernholm, and H. Babic, *Nucl. Instrum. Methods* **204,** 1 (1982).
11. M. Eriksson, *Nucl. Instrum. Methods* **203,** 1 (1982).
12. E. Rand Roy, *Recirculating Electron Accelerators* (Amsterdam, 1984).
13. K. A. Belovintsev, A. I. Karev, and V. V. Kurakin, FIAN Preprint No. 84, Moscow (1977).
14. V. K. Grishin, M. A. Sotnikov, and V. I. Shvedunov, *Phase Motion in the Microtron and Choice of Parameters of the CW Racetrack Microtron of the Institute of Nuclear Physics, Moscow State University* (Moscow, 1984); presented at the All-Union Inst. of Sci. and Techn. Information, Report No. 656–85.
15. A. A. Kolomenskii, *Sov. Theor. Phys.* **30,** 1347 (1960).
16. S. P. Kapitsa, and V. N. Melekhin, *Microtron* (Izd. "Nauka," Moscow, 1969).
17. V. N. Melekhin, *JETP Lett.* **68,** 1601 (1975).
18. V. K. Grishin, M. A. Sotnikov, and V. I. Shvedunov, Vestnik MGU **27,** 26 (1986).
19. H. Babic and M. Sedlacek, *Nucl. Instrum. Methods* **56,** 170 (1967).
20. P. K. Debenham, S. Penner, P. L. Ayres, R. L. Cufler, E. R. Lindsrom, R. E. Martin, A. Mitrs, J. M. Potter, R. R. Stokes, P. J. Iallerico, and L. Wilkerson, *IEEE Trans. Nucl. Sci.* **NS-30,** 1391 (1983).
21. M. A. Sotnikov, Thesis (Moscow, 1985).